

Jets and sprays arising from a spark-induced oscillating bubble near a plate with a hole

Karri, Badarinath; Ohl, Siew-Wan; Klaseboer, Evert; Ohl, Claus-Dieter; Khoo, Boo Cheong

2012

Karri, B., Ohl, S.-W., Klaseboer, E., Ohl, C.-D., & Khoo, B. C. (2012). Jets and sprays arising from a spark-induced oscillating bubble near a plate with a hole. *Physical Review E*, 86(3), 036309.

<https://hdl.handle.net/10356/95316>

<https://doi.org/10.1103/PhysRevE.86.036309>

© 2012 American Physical Society. This paper was published in *Physical Review E* and is made available as an electronic reprint (preprint) with permission of American Physical Society. The paper can be found at the following official DOI: [<http://dx.doi.org/10.1103/PhysRevE.86.036309>]. One print or electronic copy may be made for personal use only. Systematic or multiple reproduction, distribution to multiple locations via electronic or other means, duplication of any material in this paper for a fee or for commercial purposes, or modification of the content of the paper is prohibited and is subject to penalties under law.

Downloaded on 23 Oct 2022 16:05:52 SGT

Jets and sprays arising from a spark-induced oscillating bubble near a plate with a hole

Badarinath Karri

*NUS Graduate School for Integrative Sciences and Engineering, Center for Life Sciences, #05-01,
28 Medical Drive, Singapore 117456 and Singapore-MIT Alliance, 4 Engineering Drive 3, Singapore 117576*

Siew-Wan Ohl and Evert Klaseboer

*Institute of High Performance Computing, Agency for Science, Technology and Research, 1 Fusionopolis Way,
#16-16 Connexis, Singapore 138632*

Claus-Dieter Ohl

*School of Physical and Mathematical Sciences, Nanyang Technological University, Division of Physics and Applied Physics,
SPMS-04-01, 21 Nanyang Link, Singapore 637371*

Boo Cheong Khoo*

*Department of Mechanical Engineering, National University of Singapore, Kent Ridge, Singapore 119260 and Singapore-MIT Alliance,
4 Engineering Drive 3, Singapore 117576*

(Received 9 April 2012; published 12 September 2012)

An experimental study of jets and sprays formed by a spark-induced bubble collapsing near a plate with a hole is presented. A Perspex plate with a hole at its center is placed in a half-filled water tank with its top face near the air-water interface. A bubble is created using a low-voltage electrical spark below the hole in the plate. The bubble expands against the hole, which pushes the liquid present within the hole and leads to an initial primary jet of water that emerges from the other end of the hole into air. The bubble subsequently collapses and leads to a second jet that is characterized by short bursts of liquid spray followed by a thicker continuous liquid column. The impact of the sprays onto the primary jet leads to perturbations in the jet and the breakup of the latter into fine droplets. The entire phenomenon is recorded using a high-speed camera to visualize the mechanism both within and outside the hole. The results give a clearer indication of the mechanism behind a recently reported phenomenon on the formation of impacting jets caused by bubble expansion and collapse at the micrometer length scale. The variation of the jet characteristics with parameters such as the position of the water-air interface with respect to the plate and the hole geometry (i.e., the hole diameter and the plate thickness) is also presented.

DOI: [10.1103/PhysRevE.86.036309](https://doi.org/10.1103/PhysRevE.86.036309)

PACS number(s): 47.60.Kz, 47.40.Nm, 47.55.dp

I. INTRODUCTION

A nonequilibrium bubble oscillating near a rigid boundary is known to collapse, thereby generating a shock wave and a jet directed toward the boundary. This phenomenon has been studied traditionally for its role in cavitation damage such as to ship propellers and turbomachinery. Two possible mechanisms have been proposed for the cavitation damage, namely, (a) damage due to the high-speed jet resulting from the bubble collapse [1–4] and (b) damage due to the high pressures and shock waves generated upon bubble collapse [5–7]. In recent years, collapsing bubbles near a boundary have been studied for more useful applications such as in pumping of fluids from one side of a boundary to another through a hole at the location of jet impact [8–10], in the cleaning of surfaces using a jetting bubble [11], and in the poration of cells with potential applications in drug delivery [12,13]. In this paper we demonstrate the dynamics of an oscillating and collapsing bubble near a perforated boundary leading to the formation of two impacting jets and their breakup into a fine spray of droplets. The high-speed jet formed upon bubble collapse plays a key role in the observed phenomenon.

The formation of jets of liquid in air and their breakup characteristics have been studied for more than a century. Eggers and Villermaux [14], in a review on the physics of liquid jets, gave a historical account and described the different aspects of jet breakup including the mechanisms that lead to the breakup in various situations such as in sheets, jets, and sprays. They also presented the analytical, experimental, and numerical approaches used to study the different phenomena. For the case of a round liquid jet in a stagnant gas, Lin and Reitz [15] classified the jet breakup phenomena into four different regimes based on the dominant mechanisms leading to jet breakup. Separately, in studies on multiple jets, the impingement of two liquid jets either in a head-on collision or at an angle has also been studied both experimentally and analytically [16–20]. The collision results in a thin elliptical-shaped sheet of liquid in the plane bisecting the angle between the two jets with a rim of droplets surrounding the sheet.

In a recent study [21] we showed the formation of two jets that impact coaxially and lead to a circular liquid sheet in the plane perpendicular to the jets. The sheet had a rim of droplets and the phenomenon was observed at a length scale of micrometers. The formation of these impinging jets is driven entirely by a cavitation bubble. A shock wave from a lithotripter nucleates a cavitation bubble below a hole of a few

*mpekbc@nus.edu.sg

micrometers in diameter etched in a silicon wafer plate. The plate is located at an air-water interface and positioned such that the hole is at the focus of the lithotripter. The oscillating cavitation bubble leads to two jets: a slower primary jet during its expansion cycle, followed by a faster secondary jet formed by the bubble collapse. The interaction between the jets leads to the liquid sheet, which breaks up into a spray when a higher shock pressure is used. In that study the key drivers of the impacting jets were found to be (i) the interaction of the shock wave with the hole, which nucleates a bubble at the hole, and (ii) the ability of the bubble to actuate flow through the hole during both its expansion and collapse cycles. However, the mechanism within the hole leading to the jet impact could not be visualized or discerned. The evolution of the bubble at the bottom of the plate and the jet on top over time were also recorded in separate experiments. The mechanism of jet impact was deduced by correlating the times of the two image sequences. This was justified by the repeatability of the bubble and jet formation.

The present study is motivated by two questions arising from this earlier study [21]: (i) to determine if the formation of impacting jets using a bubble can be replicated at a larger length scale (millimeter) and (ii) to gain a deeper insight into the mechanism within the hole that led to the impacting jets. It is shown here that by a scaling up of the bubble and hole geometry to a millimeter length scale, the phenomenon of impacting jets driven by a cavitation bubble can still be realized. A Perspex plate ($80 \times 80 \text{ mm}^2$) with a thickness of 12 mm and a hole at its center was placed at the surface of water and a bubble was created using a low-voltage electrical spark below the plate. The Perspex plate is transparent and so the dynamics within the hole can be observed. The larger scale leads to slower dynamics, which is easier to observe with a high-speed camera. A high-speed video camera is used to record the bubble, the jet, and the dynamics within the hole simultaneously. The observations confirm and elaborate on the mechanism of the jet and spray formation that was deduced in the earlier study [21].

The experiments described in this paper differ from the experiments in Karri *et al.* [21] in two ways: the mechanism to create the bubble and the length scales. In the study by Karri *et al.* [21], the nucleation of the bubble was a consequence of the interaction of the shock wave with the free surface through the hole. In the experiments described in this paper, the bubble is created using a low-voltage electrical spark. A parametric study is also presented here, which shows the variation of the jet characteristics with (a) the hole geometry, i.e., hole radius and plate thickness, and (b) the position of the water-air interface with respect to the plate.

The rest of the paper is organized as follows. In Sec. II the experimental setup is described. In Sec. III a representative case study is presented. Using high-speed images, the sequence of events leading to the jet and spray formation is described. This is followed by a more detailed description of the dynamics within the hole using the same case study. The case study clearly shows the role of the bubble in the evolution of the jets. This is followed by a detailed parametric study. The details of the parameters that are varied are presented. The effect of varying these parameters (hole geometry and the position of the water-air interface) on the jetting characteristics is then

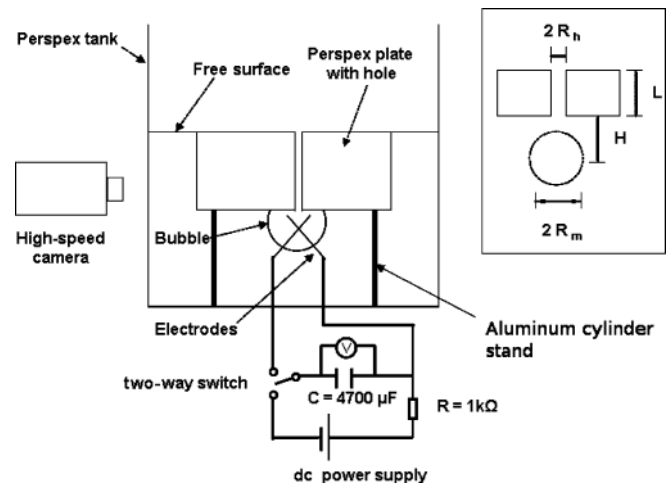


FIG. 1. Schematic of the experimental setup. The dimensions are indicated in the rectangular box on the right. Here R_m is the maximum radius of the bubble, R_h is the radius of the hole in the plate, and H is the distance between the center of the bubble and the bottom of the plate. The thickness of the plate is denoted by L .

shown through image sequences and the results are discussed. A summary is presented in Sec. IV.

II. EXPERIMENTAL SETUP AND DESCRIPTION

The schematic of the experimental setup is shown in Fig. 1. The setup consists of a tank to hold the liquid, an electrical circuit to create the spark bubble, a Perspex plate with a hole through which the jets are observed, a custom-built stand to keep the plate fixed in position, and a high-speed camera and illumination system to record the phenomenon.

The tank used is made of Perspex with dimensions of $160 \times 160 \times 160 \text{ mm}^3$. The electrical circuit used to create the spark bubble consists of a 1-k Ω resistor in series with a capacitor of 4700 μF , a two-way switch, and a pair of thin copper wires ($\sim 0.1 \text{ mm}$ in diameter) that are used as electrodes. The electrodes are crossed and placed in contact with each other and immersed in the liquid. The plates used had dimensions of $80 \times 80 \text{ mm}^2$ with a thickness of 2, 5, or 12 mm. The plate is aligned such that the hole at its center is exactly above the crossing point of the wires (or bubble center). Water was then added such that the top face of the plate is situated on the air-water interface with air on top and water below. In order to keep the plate stable during the course of the experiment, it is secured with screws at its corners to a customized stand made of four aluminium cylinders.

The experimental procedure is described as follows. The capacitor is first charged to $\sim 55 \text{ V}$ with the resistor in the circuit and then short circuited through the electrodes using the two-way switch. A spark is thus produced and a bubble comprising of gaseous products from the spark discharge and liquid vapor is formed. The distance between the bubble center and the bottom of the plate H is adjusted prior to the sparking such that H/R_m is less than 1, where R_m is the maximum bubble radius. Here H' ($= H/R_m$) denotes the nondimensional bubble center to plate distance and $H' < 1$ ensures that the bubble is in contact with the plate during its expansion cycle. As a result, the bubble displaces some

fluid from the hole during its expansion to form a primary jet, which is described in Sec. III. A high-speed camera operated at 30 000 frames per second (Photron Fastcam SA1.1 color) was used to record the bubble and jets. In the experiments both the bubble and the jet are recorded simultaneously, which gives clear evidence of the sequence of events leading to the sprays and jet impact. The setup was illuminated using a high-power lamp (ARRI, ARRISUN, maximum power 525 W) by a diffused back lighting method. After the recording, image processing operations (conversion to grayscale image, background subtraction, and contrast enhancement) were done on the images using the software ImageJ. The images give

a clear indication of the phenomenon occurring within the hole.

III. RESULTS AND DISCUSSION

A. Impacting jets through a cylindrical hole

Figures 2 and 3 show the phenomenon of jet impacts driven by an oscillating and collapsing bubble. The overall sequence of events is first described using Fig. 2. Subsequently, we focus on the dynamics within the hole in Fig. 3, using a portion of the sequence from Fig. 2 in greater detail. In Fig. 3 the background

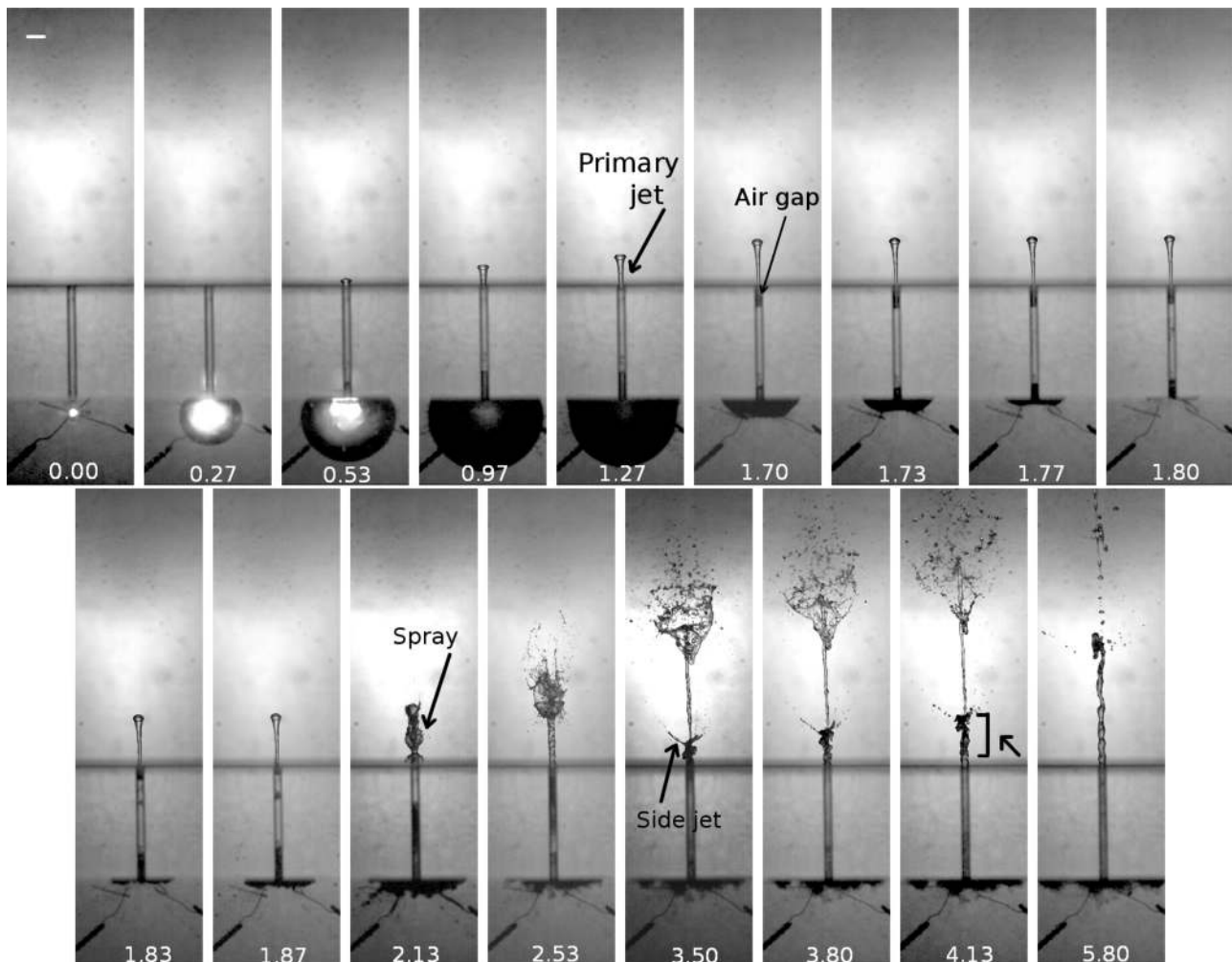


FIG. 2. Overall sequence of events leading to the formation of two impacting jets and their resultant breakup due to an oscillating bubble near a holed plate. The time (in ms) is indicated at the bottom of each frame. The plate has a thickness of $L = 12$ mm and a hole of radius $R_h = 0.5$ mm. Note the formation of an initial primary jet as the bubble expands into the hole ($t = 0.53$ and 0.97 ms) and a tapering of its bottom portion and the formation of an air gap at the top of the hole as the bubble shrinks ($t = 1.27$, 1.70 , and 1.73 ms). The bubble collapse leads to a perturbation propagating upward through the hole between $t = 1.77$ and 1.87 ms (see Fig. 3 for a zoom into the hole). The liquid present in the hole is pushed against the air gap and emerges as short spray bursts that impact on the primary jet and cause perturbations in the jet as shown at $t = 2.13$ ms (described in greater detail in Fig. 3). The primary jet subsequently breaks up into fine droplets ($t = 2.53$ – 4.13 ms) as it moves forward pushed by the fluid pumped by the collapsed bubble. A concentric jet of liquid characterized by two side jets (in the planar view) emerges later, as seen clearly at $t = 3.50$ ms. This results from expansion of the gas from the remnants of the bubble as it emerges out of the hole along with fluid. The darker color of the liquid immediately following the side jets (indicated by the arrow at $t = 4.13$ ms) is due to the bubble or electrode remnants. Later, further liquid is pumped by the bubble and comes out as a thicker continuous column ($t = 5.80$ ms). This liquid is distinct from the initial primary jet. The scale bar corresponds to a length of 2 mm. The maximum radius of the bubble obtained is $R_m = 6.3$ mm.

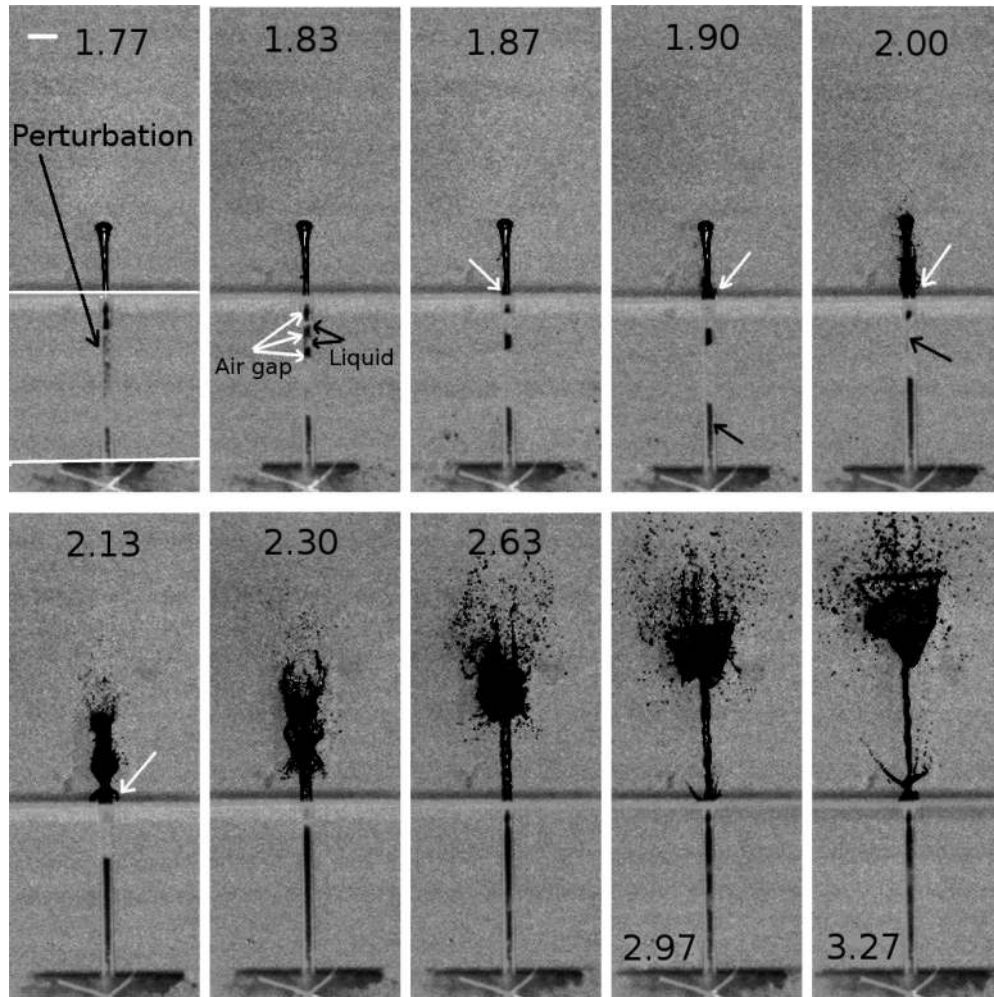


FIG. 3. Images from the case study in Fig. 2 between time $t = 1.77$ and 3.27 ms shown (with background subtracted) to get a clear picture of the mechanism within the hole subsequent to bubble collapse. The numbers in each frame indicate the time in ms. The bubble collapse at $t = 1.77$ ms leads to a perturbation propagating through the hole seen as a faint dark vertical line within the hole at $t = 1.77$ ms. Alternating air gaps (dark) and liquid packets (gray) are also formed within the hole (indicated by arrows at $t = 1.80$ ms). The collapsed bubble pumps liquid into the hole due to jetting induced upon collapse. This pumped liquid is seen as a dark line moving forward at the bottom of the hole from $t = 1.90$ ms onward (indicated by the black arrow at $t = 1.90$ ms). The pumped liquid also pushes the liquid originally present within the hole upward (gray region indicated by the black arrow at $t = 2.00$ ms). The moving liquid packets remove the air gaps and emerge in the form of short bursts of spray (formed by air-liquid interaction) and impact the primary jet as indicated at $t = 1.87, 1.90, 2.00,$ and 2.13 ms (white arrows). The impacts lead to perturbations on the jet and its breakup into fine droplets and a spray as it moves forward, being pushed by the pumped liquid ($t = 2.13$ – 3.27 ms). At $t = 2.97$ ms a concentric jet (noted as two side jets in the planar image) can be seen to emerge from the hole. This is due to the gas from the remnants of the collapsed bubble that expands as it emerges out of the hole. The scale bar corresponds to a length of 2 mm.

has been subtracted from the images to get a clearer picture of the phenomenon occurring within the hole.

In Fig. 2, time $t = 0.00$ ms shows the instant when the spark below the plate with the hole is first observed and the bubble starts expanding. As the bubble expands, part of the bubble moves into the hole, as seen at times $t = 0.53$ and 0.97 ms. The expanding bubble pushes some of the liquid within the hole, which is ejected from the other side of the hole as a primary jet. The primary jet is first observed on top of the plate at time $t = 0.53$ ms. When the bubble expands, this jet moves upward until $t = 0.97$ ms. The velocity of this primary jet is calculated to be 3.5 m/s between $t = 0.53$ and 1.70 ms. The bubble reaches its maximum size of $R_m = 6.3$ mm at $t = 0.97$ ms and then shrinks, reaching a minimum volume and collapsing

at $t = 1.77$ ms. As the bubble starts to shrink, the bubble pulls the liquid in the hole toward the bottom of the hole (due to backflow). Consequently, the bottom part of the primary jet starts to taper and the jet acquires a conical shape with a broader top ($t = 1.27$ ms). The shrinkage of the bubble and the backflow result in the formation of an air gap in the hole below the tapered portion of the primary jet, as seen at $t = 1.70$ and 1.73 ms. Between $t = 1.77$ and 1.87 ms, the activity is mainly within the hole, which is described in the following paragraph. During the period from $t = 1.77$ to 3.50 ms, the collapsed bubble pumps liquid through the hole due to the jetting induced upon collapse. This resultant jet is characterized by a series of short liquid packets that emerge in the form of bursts of spray, impact on the primary jet, and lead to perturbations on the

jet and its breakup. This is followed by a thicker continuous column of liquid. The developed perturbations on the primary jet due to the impact by the liquid packets can be observed in the image at $t = 2.13$ ms. The pumped liquid inside the hole causes the perturbed primary jet to move upward as shown in the period from $t = 2.53$ to 4.13 ms. The primary jet breaks up into fine droplets and a spray during this period. The impact of the sprays also accelerates the jet tip and its velocity is estimated to be around 25 m/s after the impact. In the frame at $t = 3.50$ ms, a concentric jet observed as two small side jets in the planar view is also shown. It is suggested here that this concentric jet is due to the expanding gas from the remnants of the collapsed bubble as the gas emerges on top of the hole together with the liquid. This is supported by the observation that the two side jets and the liquid immediately following it ($t = 3.50$ – 4.13 ms) are black in color as compared to the lighter column just before the side jets ($t = 2.53$ ms) and subsequently following them ($t = 5.80$ ms). Between $t = 3.50$ and 5.80 ms, a thicker column of liquid can also be observed on top of the hole following the side jets. This column can be clearly distinguished from the primary jet in the frames at $t = 4.13$ – 5.80 ms.

Through Fig. 3 we now focus in greater detail on the dynamics within the hole and the sequence of events that lead to the breakup of the primary jet into a spray and the subsequent thicker column of liquid. We use the same case study as shown in Fig. 2, but include more frames during the period $t = 1.77$ – 3.27 ms. The images are shown after background subtraction. The plate is identified by the solid white horizontal lines in the first frame of the sequence. In Fig. 3 the first frame ($t = 1.77$ ms) shows the situation within the hole at bubble collapse. In this frame, in addition to the air gap (dark gap) at the top of the plate, a perturbation resulting from the bubble collapse can be seen propagating through the hole as noted by a faint dark vertical line inside the hole. Subsequently alternating dark (air pockets) and gray (water) gaps are observed in the top half of the hole at $t = 1.80$ ms. The water gaps are henceforth termed liquid packets. It can be observed that as each of the three air pockets get removed due to the moving liquid packets within the hole, it results in a series of short bursts of spray at the top of the hole as indicated in the frames at $t = 1.83$, 1.87 , 1.97 , and 2.13 ms. The formation of the sprays is due to the interaction of the liquid packets with the air gaps as the liquid packets emerge on top of the hole. At $t = 2.00$ ms, the removal of the final air gap results in the emergence of a spray with an umbrellalike top as seen at $t = 2.13$ ms. The impact of the spray bursts with the primary jet leads to perturbations in the primary jet and its subsequent breakup into fine droplets as seen from $t = 2.13$ to 3.27 ms. After $t = 2.13$ ms, there are no visible air gaps inside the hole and the liquid emerges on top of the hole as a continuous column between $t = 2.13$ and 2.97 ms. The continuous liquid flow, which is noted as an advancing dark line at the bottom half of the hole from $t = 1.80$ to 2.63 ms, is caused by the pumping of liquid by the collapsed bubble. It should be noted here that this pumped liquid is distinct from the liquid initially present within the hole, which is the gray region above the darker advancing liquid column as indicated by a black arrow at $t = 2.00$ ms. At $t = 2.97$ ms, the nature of the liquid emerging from the hole changes with two side

jets observed in this planar view, which is attributed to the expanding gas from the remnants of the bubble as described earlier.

Based on the above sequences, the mechanism leading to the formation of the impacting jets and the resultant spray is summarized as follows. A bubble expanding in close proximity $H' < 1$ to a plate with a hole situated at an air-water interface pushes part of the liquid within the hole to emerge as a primary jet on the other side of the hole. The primary jet continues to move upward as the bubble expands and reaches its maximum size. The bubble then begins to shrink, leading to a backflow within the hole. Consequently, although the primary jet continues to translate upward, it acquires a conical shape with a narrower bottom and a broader top portion. By the time the bubble reaches its minimum volume, the backflow results in the formation of an air gap at the top of the hole just below the bottom (now narrowed down) portion of the primary jet. The bubble then collapses, leading to a perturbation that travels as a disturbance within the hole. The perturbation results in the formation of alternating air gaps and liquid packets near the top half of the hole. The bubble collapse also leads to pumping of fluid through the bottom half of the hole. This perturbation and the pumping of fluid due to bubble collapse leads to two effects. First, as the liquid within the hole moves forward, the air gaps are removed by the interspaced liquid packets. The interaction of the liquid packets with the air gaps results in the breakup of the liquid into a series of short bursts of spray as the liquid packets emerge on top of the hole. The impact of these spray bursts at the bottom of the primary jet cause perturbations in the jet. This results in a breakup of the jet into fine droplets and a spray even as it moves forward, pushed by the liquid pumped from below. Second, the fluid that is pumped through the hole by the collapsed bubble emerges as a thicker continuous jet of liquid on top of the hole following the spray.

B. Parametric study

After getting insight into the mechanism that leads to the formation of impacting jets due to an oscillating bubble, a parametric study was conducted. The parameters that are expected to affect the bubble and jet characteristics were first identified as the hole radius R_h , the maximum bubble radius R_m , the distance of the bubble from the bottom of the plate H , and the plate thickness L . These parameters are indicated on the top right in Fig. 1. Using the spark-discharge method to create the bubble, precise control over the bubble size is limited because of the difference in voltage discharged during the short-circuiting process, which may vary from 4 to 7 V. The bubble center to plate distance H was also always chosen such that $H' < 1$ to ensure that the bubble will expand against the hole during its expansion cycle. Thus only the two parameters related to the plate are varied. The first parameter is the plate thickness L . Plates of three different thicknesses $L = 2, 5$, and 12 mm were used to study the effect of plate thickness. For all three plates, the hole radius was kept fixed at $R_h = 1$ mm. The second parameter that is varied is the radius of the hole R_h . In this case, the plate thickness was fixed at $L = 12$ mm for all the plates used. Seven different plates with hole radii of $R_h = 0.5, 1, 3, 6, 7.5, 9$, and 12 mm were chosen for this parametric study.

The values of L and R_h were chosen based on two dimensionless parameters, namely, aspect ratio $L/2R_h$ and the ratio of bubble radius to hole radius R_m/R_h . In the earlier study by Karri *et al.* [21], the diameter of the hole in the plate was $2R_h \sim 25 \mu\text{m}$ and the plate had a thickness L of around $500 \mu\text{m}$. This indicates a high aspect ratio $L/2R_h$ of $\sim 20:1$, which resulted in the impacting jets. The present experiments

confirm that the formation of impacting jets needs a high aspect ratio $L/2R_h$, which was around 12 in the base case (Fig. 2). As the ratio is reduced (due to decrease in L or increase in R_h), the impacting jets with a spray are not so prominent or are even absent in some cases (see, for example, results from Fig. 4). A second dimensionless parameter that plays a role in the jet characteristics is the bubble size to hole size ratio

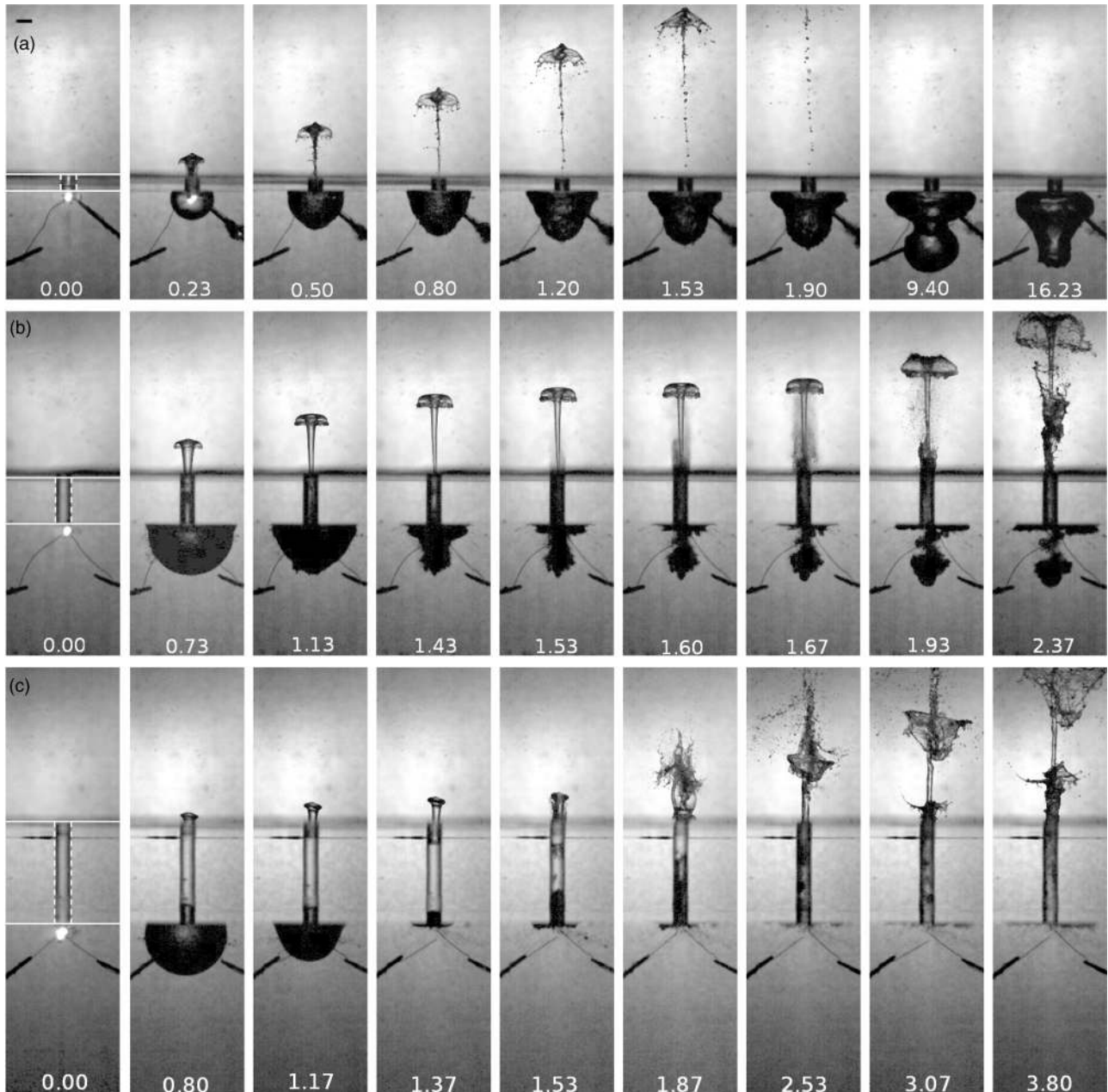


FIG. 4. Effect of varying the plate thickness on the characteristics of the jet and the bubble at the bottom. The plates used here have thicknesses of (a) $L = 2 \text{ mm}$, (b) $L = 5 \text{ mm}$, and (c) $L = 12 \text{ mm}$. The hole radius is $R_h = 1.0 \text{ mm}$ in all the plates. The water level within the hole in all the cases is coincident with the top face of the plate. In (a) note the total ejection of the liquid in the hole due to the bubble expansion ($t = 0.80 \text{ ms}$). The subsequent bubble dynamics is different from that of a submerged nonequilibrium bubble. The maximum bubble radius is $R_m = 3.9 \text{ mm}$. In (b) the bubble splits into two upon collapse. The jet characteristics are similar to that of Fig. 2 but driven by the top half of the split bubble. The bottom portion of the split bubble moves away from the plate. The maximum bubble radius $R_m = 5.3 \text{ mm}$ in this case. In (c) both the jet and bubble characteristics are similar to that in Fig. 2. The primary jet, the spray impacting the jet, and the subsequent continuous liquid column are thicker here due to the larger hole radius used as compared to Fig. 2. The bubble reaches a maximum radius $R_m = 5.1 \text{ mm}$. The scale bar corresponds to a length of 2 mm .

R_m/R_h . In the study by Karri *et al.* [21], the bubble radius varied from a value of 140 to 270 μm , which corresponds to a R_m/R_h value varying from ~ 5.6 to 11. In other words, the bubble should be much larger than the hole to displace liquid from the hole as it expands. In the present experiments, the bubble radius R_m varies between 3 and 6 mm. It is indeed seen that the impacting jets are prominently observed at low hole radii R_h . As the hole radius R_h increases, the volume of liquid displaced by the bubble relative to the volume within the hole decreases and so the initial jet due to bubble expansion becomes weaker (see results from Sec. III E).

The formation of the impacting jets depends on the presence of liquid within the hole during the bubble expansion and collapse. Therefore, the position of the air-water interface and the level of water within the hole are expected to affect the jet characteristics. Consequently, a study of the effect of water level was also carried out. Four different positions of the water-air interface relative to the plate were studied: (i) The plate is positioned with its top face coinciding with the water level, with air on top of the plate and water below (default position); (ii) the plate is completely submerged with a 0.5-mm-thick layer of water on top of the plate; (iii) the plate is submerged halfway through its thickness; and (iv) the bottom of the plate is situated just above the water level and in contact with it. The water level positions (ii)–(iv) are indicated in the first frames of the sequences shown in Figs. 5(a)–5(c) using a dash-dotted horizontal line. The plate used in these experiments had $R_h = 0.5$ mm and a thickness $L = 12$ mm.

We now discuss the results from the parametric study by varying the parameters as described above.

C. Effect of plate thickness L on jet and bubble characteristics

Figure 4 shows the effect of varying the plate thickness L on the characteristics of the jet and the bubble. The thickness of the plate used is $L = 2, 5,$ and 12 mm, respectively, for Figs. 4(a), 4(b), and 4(c). The plate used had a hole of radius $R_h = 1$ mm in all three cases. The position of the plate (solid white horizontal lines) and the hole (dotted white vertical lines) are shown in the first frame of each sequence ($t = 0.00$ ms) when the spark is first observed. The water level within the hole in all the cases is coincident with the top face of the plate.

In Fig. 4(a) the bubble and the primary jet due to the expanding bubble are shown at $t = 0.23$ ms. The bottom of the primary jet starts to narrow and the jet assumes an umbrella shape between $t = 0.23$ and 1.53 ms. The velocity of the jet is calculated to be 6.9 m/s. In this case, due to the small thickness of the plate, the bubble pushes out the entire fluid within the hole during its expansion to a maximum radius of $R_m = 3.9$ mm. Consequently, as the jet moves upward, for example, at $t = 0.80$ ms, the bubble is vented to the outside air and experiences air on one side and water on the other. The subsequent bubble dynamics is much different from an oscillating nonequilibrium bubble in liquid. The bubble starts to split in the middle ($t = 1.20$ – 9.40 ms), but eventually the splitting is not complete and the bottom portion of the bubble merges with the top portion as seen at $t = 16.23$ ms. No spray or a subsequent continuous liquid column is observed in this case as the hole consists of only air and no liquid after the formation of the primary jet. The dynamics of the

vented bubble, particularly its tendency to split, resembles the dynamics of a cavity formed at a free surface due to impact of a solid object or disk [22,23], where the cavity collapse is driven by hydrostatic pressure. In the earlier studies above, the cavity is exposed on one side entirely to the free surface. whereas in the present experiments, the bubble is vented through a small hole. The splitting is also incomplete here and does not form two oppositely directed jets, unlike in the earlier reported experiments [22,23].

When a plate of intermediate thickness $L = 5$ mm is used [Fig. 4(b)], the bubble expands to its maximum radius of $R_m = 5.3$ mm by $t = 0.73$ ms. A primary jet with a narrower base and an umbrella-like top is seen at this time. In Fig. 2 the bottom of the primary jet was observed to narrow due to backflow during bubble shrinkage. A similar observation is made here from $t = 0.73$ to 1.43 ms. The velocity of the primary jet is calculated to be 3.9 m/s. At $t = 1.53$ ms, the bubble collapses. An interesting phenomenon is observed as the bubble collapses: The bubble splits into two with the top portion leading to a perturbation and spray through the hole ($t = 1.53$ – 1.67 ms) while the bottom portion moves in the opposite direction away from the plate. At $t = 1.93$ and 2.37 ms, a thicker continuous column of liquid following the spray is also observed. The phenomenon on top of the plate is quite similar to that in Fig. 2. In this case though, the primary jet has a distinct umbrella-shaped top and the spray appears to impact against the primary jet but does not change its character, much as seen from the images at $t = 1.67, 1.93,$ and 2.37 ms.

Figure 4(c) shows the bubble near a plate of thickness $L = 12$ mm. The bubble reaches its maximum radius of $R_m = 5.1$ mm at $t = 0.80$ ms and its minimum volume at $t = 1.37$ ms. A primary jet is seen to emerge on top of the plate from $t = 0.80$ to 1.37 ms at a velocity of 1.6 m/s. As the bubble collapses ($t = 1.53$ ms), a liquid emerges in the form of a spray and impacts the primary jet. The spray also accelerates the jet tip and leads to its breakup ($t = 1.53$ – 3.80 ms). The velocity of the jet tip after the impact of the spray is calculated to be 8.7 m/s. Subsequently, a thicker column of liquid is observed ($t = 3.07$ and 3.80 ms) following the spray. Side jets can also be distinguished at the top of the thicker column ($t = 3.07$ ms) attributed to the gas from the bubble remnants expanding as it emerges. The phenomenon observed is very similar to that observed in Fig. 2 except that in this case, a larger hole is used ($R_h = 1$ mm).

Thus the plate thickness does have an effect on the jet characteristics. The results show that formation of the impacting jets requires that the plate should be thick enough so that the bubble does not vent to the atmosphere as it expands. In this case, the bubble is fully vented when $L = 2$ mm, which is the smallest thickness used.

D. Effect of water level on the jet characteristics

Next we investigated if the location of the air-water interface with respect to the plate plays a role in the jet characteristics. In all the cases described until now (Figs. 2–4), the water level was coincident with the top face of the plate. In this parametric study, three different cases were studied as shown in Figs. 5(a)–5(c): (a) The water level is located 0.5 mm above the plate, i.e., the plate is fully submerged; (b) the water level

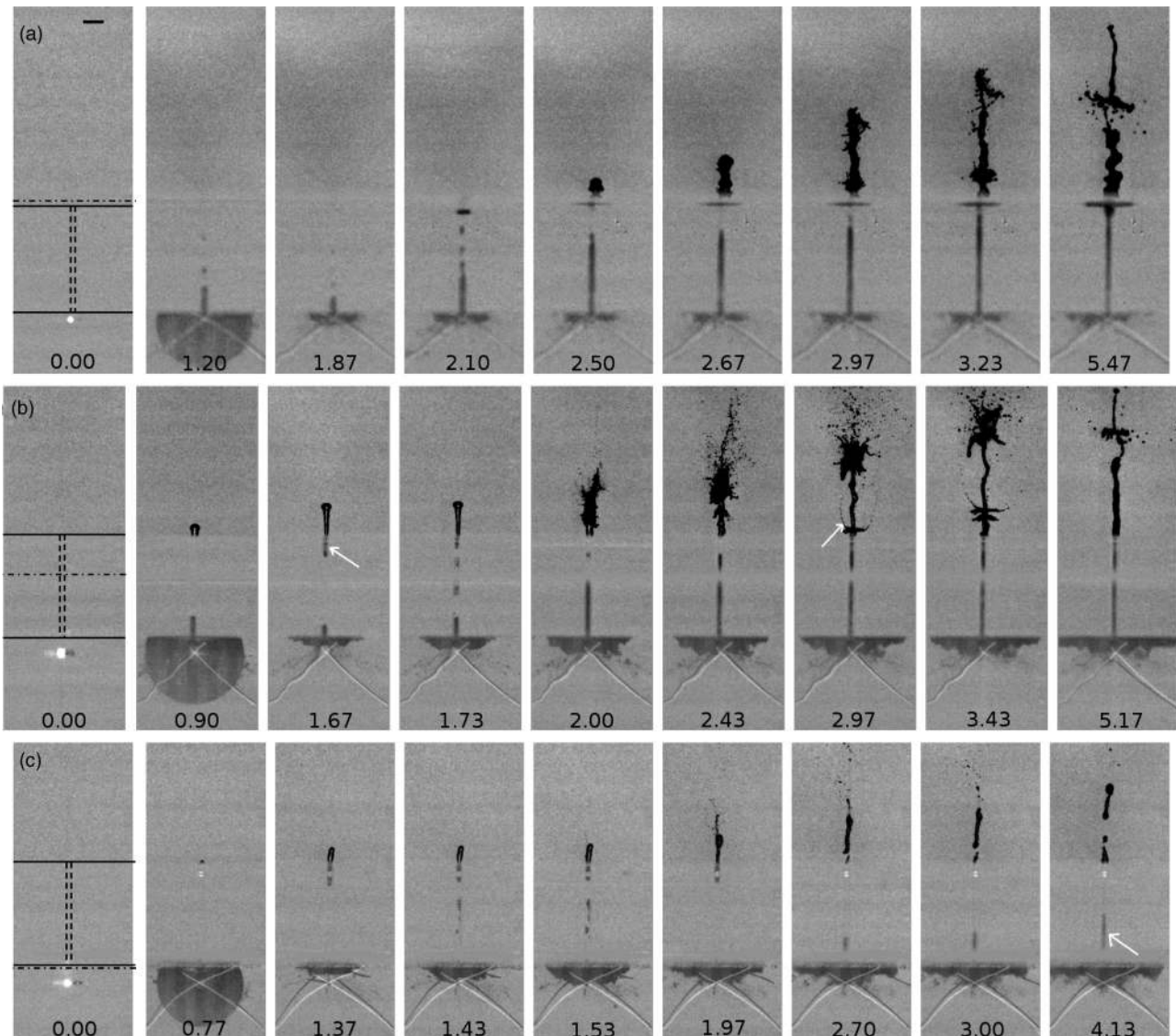


FIG. 5. Effect of varying the water level with respect to the plate on the jet characteristics (a)–(c). The images are shown after background subtraction. The plate used had a thickness of $L = 12$ mm and hole radius of $R_h = 0.5$ mm. The water level is indicated with a dash-dotted horizontal line: (a) plate just submerged, (b) plate half submerged, and (c) plate just above the water surface. Note the absence of the primary jet due to bubble expansion in (a). The maximum radius of the bubble was $R_m = 5.6$ mm. In (b) the sequence of events is similar to that in Fig. 2. The air gap is indicated by a white arrow at $t = 1.67$ ms. The side jets are also indicated at $t = 2.97$ ms (white arrow). The maximum bubble radius attained was $R_m = 5.7$ mm. In (c) the bubble expansion pushes some liquid into the hole and causes it to come out as a primary jet ($t = 0.77, 1.37, 1.43,$ and 1.53 ms). A faint spray impacting the primary jet could be distinguished upon bubble collapse ($t = 1.97$ ms). A small amount of fluid is subsequently pumped through the hole by the jet induced by the collapsed bubble, which can be seen as a faint vertical line at the bottom of the hole at $t = 4.13$ ms (indicated by the white arrow). The maximum bubble radius obtained was $R_m = 5.0$ mm. The scale bar corresponds to a length of 2 mm.

is located approximately halfway through the thickness of the plate; and (c) the water level is located just below the plate and touching it. The images are shown after background subtraction to get a clearer picture of the phenomenon within the hole. The first frame in each sequence shows the positions of the plate (horizontal solid lines), the hole (vertical dotted lines), and the water level (horizontal dash-dotted line). The first frame ($t = 0.00$) is taken at the time when the spark is first observed.

In the sequence in Fig. 5(a), the bubble expands to its maximum radius of $R_m = 5.6$ mm at $t = 1.20$ ms and

collapses to its minimum at $t = 1.87$ ms. During this expansion and collapse cycle of the bubble, the bubble expands into the hole ($t = 1.20$ ms), but there is no distinguishable primary jet observed on top of the plate pushed by the expanding bubble. This is different from the case in Fig. 2 when the water level was coplanar with the top of the plate. It is possible that the liquid pushed by the expanding bubble in the form of a supposedly primary jet is diffused into the surrounding thin liquid layer on top of the plate. On the collapse of the bubble, a perturbation can be observed to propagate within the hole ($t = 2.10$ ms). As the collapsed bubble subsequently pumps

liquid through the hole, a jet is seen to emerge on top of the liquid surface into air from $t = 2.50$ to 5.47 ms. There is no prominent spray observed possibly because the formation of a spray requires the presence of both air gap (or gaps) and liquid packets within the hole. The air gap is not formed here due to the thin layer of water on top of the plate.

The sequence in Fig. 5(b) shows the bubble near a plate with the water level midway through the thickness of the plate. As the bubble expands to its maximum radius of $R_m = 5.7$ mm ($t = 0.90$ ms) and collapses to a minimum ($t = 1.67$ ms), a primary jet emerges. The jet then narrows at its bottom even as the jet tip moves forward at a velocity of ~ 2.5 m/s. An air gap (indicated by a white arrow) is also formed due to the shrinkage of the bubble and the resultant backflow at $t = 1.67$ ms. A perturbation can be seen propagating upward within the hole at $t = 1.73$ ms characterized by alternating air gap (dark) and liquid packet (gray) regions within the hole. The perturbed primary jet due to the impact of the spray burst (or bursts) can be seen clearly at $t = 2.00$ ms. The subsequent evolution of the perturbed jet and its breakup can be seen from $t = 2.00$ to 3.43 ms. During this period, the continuous liquid column due to pumping in the hole by the collapsed bubble following the spray is also noted. The side jets attributed to the gas from the remnants of the bubble are also distinguished at $t = 2.97$ ms (indicated by a white arrow). The phenomenon observed is very similar to that in Fig. 2.

The sequence in Fig. 5(c) depicts the situation where the water level coincides with the bottom of the plate. The bubble expands to its maximum radius of $R_m = 5.0$ mm by $t = 0.77$ ms. A faint semblance of a primary jet is seen on top of the plate at this time. After the bubble collapses to a minimum ($t = 1.37$ ms), a perturbation propagating upward can be observed in the hole. This is noted from the alternating movement of air and liquid between $t = 1.43$ and 1.53 ms, which leads to a faint spray. The spray impacts on the jet, leading to a slightly perturbed primary jet observed on top of the plate at $t = 1.97$ ms. By $t = 4.13$ ms, a faint dark vertical line can be observed moving forward at the bottom of the hole, which is associated with the liquid being pumped by the bubble collapse.

E. Effect of hole radius R_h on the jet characteristics

Finally, we present the effect of varying the radius of the hole in the plate R_h on the jet characteristics. Here we present six image sequences in Figs. 6(a)–6(f) with hole radii of $R_h = 2.0, 3.0, 6.0, 7.5, 9.0,$ and 12.0 mm, respectively. All the plates had a thickness of $L = 12$ mm. The images are shown after background subtraction to observe the dynamics within the hole clearly. In the first frame in each sequence, the position of the plate (solid black lines) and the hole (dotted black lines) are indicated. The water level was coincident with the top face of the plate in all cases. It should be noted here that in Figs. 2 and 4(c) two other hole radii of $R_h = 0.5$ mm and 1.0 mm have already been discussed. The characteristics of the jet and the mechanism observed in these two cases are very similar.

Figure 6(a) shows the jetting through a plate with a hole of radius $R_h = 2.0$ mm driven by the bubble. The bubble is created at $t = 0.00$ ms and reaches its maximum radius of $R_m = 4.1$ mm by $t = 0.77$ ms. A faint primary jet is also seen on top of the plate at this time. The bubble shrinks to its

minimum volume by $t = 1.43$ ms and at this time, the jet on top can be clearly seen. The velocity of the primary jet is calculated to be 4.5 m/s. The air gap within the hole due to backflow is also observed similar to that explained in earlier cases (for example, Fig. 2). At $t = 1.47$ ms, the bubble collapses and a disturbance can be seen propagating upward through the hole. A burst of spray due to the bubble collapse and the liquid packet within the hole being pushed against the air gap is first observed on top of the plate at $t = 1.67$ ms. The subsequent evolution of the perturbed jet and its breakup into a fine spray is also seen from $t = 2.33$ to 2.77 ms. By $t = 3.87$ ms the resulting fluid flow from the fluid pumped by the collapsed bubble emerges on top of the plate as a thicker jet. Here, due to the larger hole radius as compared to Fig. 2, the mass of the liquid packet forming a burst of spray and impacting the primary jet is larger, leading to a more prominent breakup of the jet. The thicker liquid column continues to move upward as seen at time $t = 6.47$ ms. The overall sequence of evolution of the jet does not differ much from the cases with $R_h = 0.5$ mm (Fig. 2) and $R_h = 1$ mm [Fig. 4(c)].

We now focus on the evolution of the jet at diameters of $R_h = 3.0, 6.0,$ and 7.5 mm as shown in Figs. 6(b), 6(c), and 6(d), respectively. The jet in the three cases shares some similarities, which are highlighted below. In all three cases, the bubble reaches its maximum radius of $R_m = 3.5, 4.7,$ and 5.5 mm, respectively, at times $t = 0.60, 0.73,$ and 0.80 ms for Figs. 6(b), 6(c), and 6(d). There is only a very weak or hardly visible primary jet observed on top of the plate for the three cases ($t = 0.60, 0.73,$ and 0.80 ms, respectively). This is possibly because the expansion of the bubbles is not strong enough to displace enough volume of fluid from the hole. However, as the bubble shrinks to its minimum volume, an air gap is formed on top of the hole for all the three cases ($t = 1.10, 1.23,$ and 1.30 ms, respectively). Subsequently, the bubble collapses and as the liquid within the hole interacts with the air gap, an initial burst of spray and a subsequent thicker liquid column can be seen for all three cases. For Fig. 6(b) the spray is observed to evolve into a crown type of structure before the thicker column of liquid catches up ($t = 1.43$ – 5.60 ms). In a similar fashion, the thicker liquid column catches up with the spray, which breaks up into fine droplets on top of the plate for the other two cases [from $t = 4.80$ to 14.73 ms for Fig. 6(c) and $t = 5.47$ and 10.23 ms for Fig. 6(d)]. The key observation from these cases is that at increased hole radius R_h with respect to the bubble radius R_m , the primary jet is weak or almost suppressed because of insufficient energy in the expanding bubble to push the liquid out of the hole.

In Fig. 6(e) an interesting observation is made. The plate used had a hole of radius $R_h = 9$ mm in this case. The bubble is created at $t = 0.00$ ms and reaches a maximum radius of $R_m = 2.7$ mm at $t = 0.33$ ms. Subsequently, it shrinks to a minimum by $t = 0.60$ ms. However, after that, the bubble does not form a jet but continues to oscillate almost spherically, reaching again a maximum at $t = 0.70$ ms. At a much later time ($t = 3.17$ ms), the bubble is observed to be almost stationary in terms of translated distance. The reason for such a behavior of the bubble is explained as follows. As the hole diameter with respect to the bubble radius increases, the bubble is subject to two opposing influences that determine the direction of the jet. Due to the presence of the plate, the bubble tends to jet upward

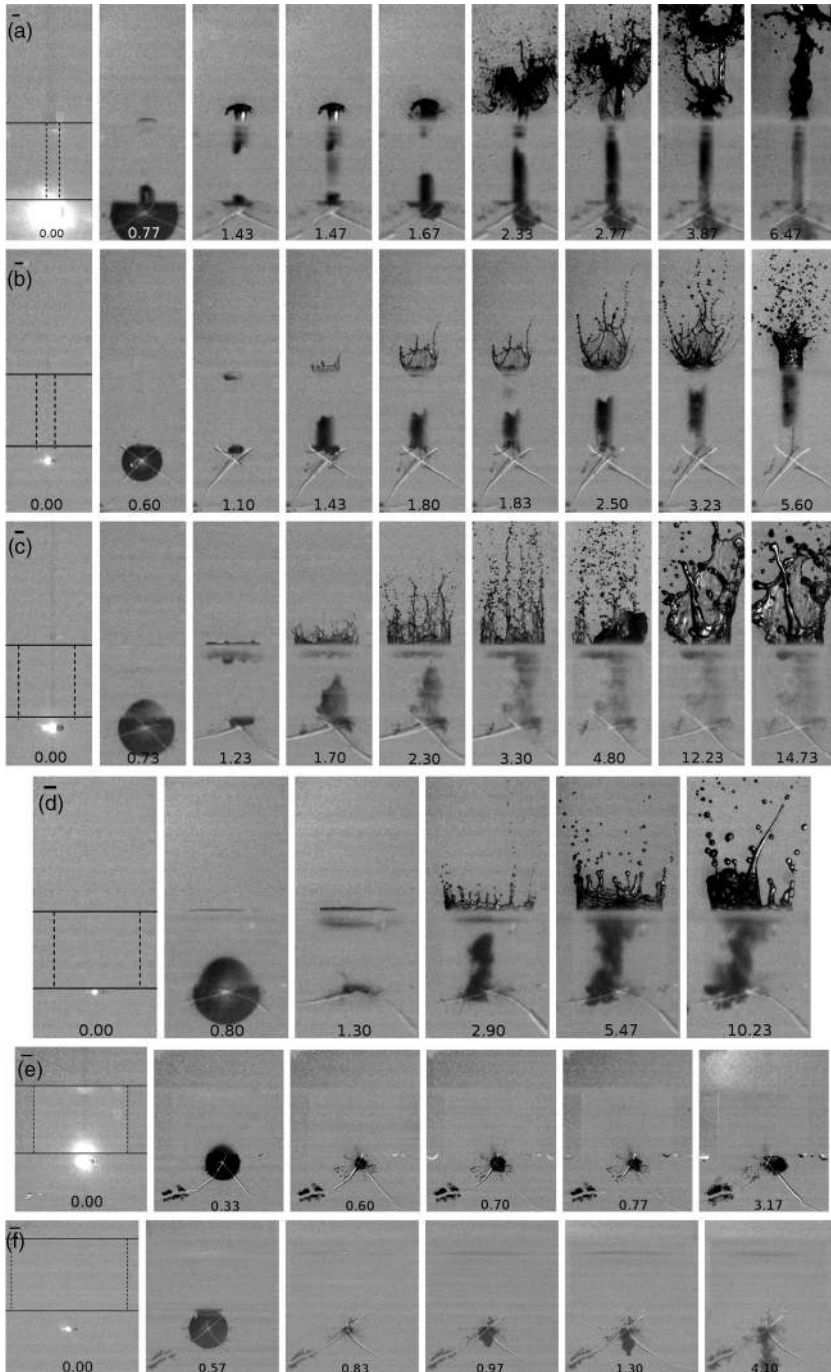


FIG. 6. Effect of varying the hole radius R_h in the plate on the jet characteristics. The images are shown after background subtraction. The hole radii used and the bubble maximum radii attained are, respectively, (a) $R_h = 2.0$ mm and $R_m = 4.1$ mm, (b) $R_h = 3.0$ mm and $R_m = 3.5$ mm, (c) $R_h = 6.0$ mm and $R_m = 4.7$ mm, (d) $R_h = 7.5$ mm and $R_m = 5.5$ mm, (e) $R_h = 9.0$ mm and $R_m = 2.7$ mm, and (f) $R_h = 12.0$ mm and $R_m = 3.1$ mm. In (a) the sequence is similar to that of Fig. 2 with a primary jet (from $t = 0.77$ to 1.47 ms), a subsequent spray impacting the primary jet and perturbing it (from $t = 1.67$ to 2.77 ms), and finally the continuous thicker liquid column through the hole (from $t = 3.87$ and 6.47 ms). (b)–(d) show a similar behavior: The bubble first expands into the hole but only a very weak or hardly visible primary jet is distinguishable. This is due to the large volume of liquid in the hole (due to large R_h) relative to the volume displaced by the bubble. During bubble shrinkage, an air gap is formed on top of the hole in all three cases [$t = 1.10$ ms in (b), $t = 1.23$ ms in (c), and $t = 1.30$ ms in (d)]. A crownlike structure is observed on top of the hole in all three cases upon bubble collapse (due to spray impact with primary jet). In (e) the bubble collapses and oscillates almost spherically. Due to the large hole radius R_h , the presence of the plate and the free surface simultaneously near the bubble leads to opposing influences on the bubble to form a jet and the bubble simply oscillates. In (f) the bubble behaves as if near a free surface and forms a jet away from the plate. All the plates used had a thickness of $L = 12$ mm. The scale bar in the first frame of each sequence corresponds to a length of 2 mm.

toward the plate. At the same time, because of the large R_h , the influence of the free surface also acts on the bubble. The free surface causes the bubble to jet away from the surface (i.e., in the downward direction). It appears that at the combination of hole radius, bubble radius, and distance H in Fig. 6(e), both the opposing influences counteract each other almost equally, resulting in a near-spherical bubble oscillation.

In Fig. 6(f) the influence of the free surface on the bubble is more clearly seen when a larger hole of $R_h = 12$ mm is used. The bubble is created at $t = 0.00$ ms and reaches a maximum radius of $R_m = 3.1$ mm at $t = 0.57$ ms and subsequently its minimum volume at $t = 0.83$ ms. However, after that, the bubble jets away from the free surface and a trail is seen to

move away from the hole ($t = 0.97$, 1.30 , and 4.10 ms). Thus an increase of the hole radius R_h of the plate leads to a variety of jetting phenomena, as evidenced by the results of Fig. 6.

IV. CONCLUSION

In this paper a further elucidation of a recently reported phenomenon of impacting jets driven by an expanding and collapsing bubble is presented. It is shown that bubble-driven jet impacts and sprays can also be replicated at a larger length scale of millimeters by suitable scaling of the bubble and the plate geometry. The mechanism behind the jets, particularly the dynamics within the hole, are now observed by using a

transparent Perspex plate and high-speed photography. The correlation between the bubble and the jetting and spray formation on top of the plate is also clearly established by recording both the bubble and the jet together in the same frame. Finally, the larger length scale of the experiment as compared to the earlier study [21] and the simple experimental setup to create a bubble enabled a detailed parametric study. The effect of the hole geometry, such as the hole diameter and the plate thickness as well as the water level in the hole, on the evolution of the jet characteristics and the bubble were studied. The bubble ejects the entire fluid within the hole and vents to the outside air when the plate thickness is small. This leads to a splitting of the bubble into two and its dynamics are different from a submerged nonequilibrium bubble in liquid. The jet characteristics also change due to this change in the bubble

character. The location of the water-air interface with respect to the plate influences the jet characteristics. For the impacting jets to form, the presence of liquid within the hole is crucial and the water level needs to be halfway or coplanar with the plate. As the radius of the hole increases, the volume displaced by the bubble during its expansion relative to the volume within the hole decreases. This leads to a weak or almost suppressed primary jet. However, an air gap is nevertheless formed upon shrinkage of the bubble. The liquid pumped by the collapsing bubble leads to a crownlike structure. At very large hole radii, the bubble jets away from the plate as if near a free surface of water. The results indicate a method for the formation, acceleration, and breakup of a jet into fine sprays by using an oscillating and collapsing bubble and could be useful for applications involving atomization of liquids.

-
- [1] M. Kornfeld and L. Suvorov, *J. Appl. Phys.* **15**, 495 (1944).
 [2] C. F. Naudé and A. T. Ellis, *Trans. ASME Ser. D* **83**, 648 (1961).
 [3] T. B. Benjamin and A. T. Ellis, *Philos. Trans. R. Soc. London A* **260**, 221 (1966).
 [4] M. S. Plesset and R. B. Chapman, *J. Fluid Mech.* **47**, 283 (1971).
 [5] N. D. Shutler and R. B. Mesler, *Trans. ASME Series D* **87**, 511 (1965).
 [6] A. Philipp and W. Lauterborn, *J. Fluid Mech.* **361**, 75 (1998).
 [7] Y. Tomita and A. Shima, *J. Fluid Mech.* **169**, 535 (1986).
 [8] B. C. Khoo, E. Klaseboer, and K. C. Hung, *Sensors Actuat. A* **118**, 152 (2005).
 [9] K. S. F. Lew, E. Klaseboer, and B. C. Khoo, *Sensors Actuat. A* **133**, 161 (2007).
 [10] B. Karri, K. S. Pillai, E. Klaseboer, S.-W. Ohl, and B. C. Khoo, *Sensors Actuat. A* **169**, 151 (2011).
 [11] C.-D. Ohl, M. Arora, R. Dijkink, V. Janve, and D. Lohse, *Appl. Phys. Lett.* **89**, 074102 (2006).
 [12] C.-D. Ohl, M. Arora, R. Iking, N. de Jong, M. Versluis, M. Delius, and D. Lohse, *Biophys. J.* **91**, 4285 (2006).
 [13] G. N. Sankin, F. Yuan, and P. Zhong, *Phys. Rev. Lett.* **105**, 078101 (2010).
 [14] J. Eggers and E. Villermaux, *Rep. Prog. Phys.* **71**, 036601 (2008).
 [15] S. P. Lin and R. D. Reitz, *Annu. Rev. Fluid Mech.* **30**, 85 (1998).
 [16] N. Dombrowski and P. C. Hooper, *J. Fluid Mech.* **18**, 392 (1964).
 [17] M. F. Heidmann, R. J. Priem, and J. C. Humphrey, Lewis Flight Propulsion Laboratory, National Advisory Committee for Aeronautics Technical Note 3835, 1957 (unpublished), http://ntrs.nasa.gov/archive/nasa/casi.ntrs.nasa.gov/19930084568_1993084568.pdf.
 [18] N. Bremond and E. Villermaux, *J. Fluid Mech.* **549**, 273 (2006).
 [19] J. C. P. Huang, *J. Fluid Mech.* **43**, 305 (1970).
 [20] G. Taylor, *Proc. R. Soc. London Ser. A* **259**, 1 (1960).
 [21] B. Karri, S. R. G. Avila, Y. C. Loke, S. J. O'Shea, E. Klaseboer, B. C. Khoo, and C.-D. Ohl, *Phys. Rev. E* **85**, 015303(R) (2012).
 [22] R. Bergmann, D. van der Meer, S. Gekle, A. van der Bos, and D. Lohse, *J. Fluid Mech.* **633**, 381 (2009).
 [23] H. N. Oguz, A. Prosperetti, and A. R. Kolani, *J. Fluid Mech.* **294**, 181 (1995).